Dynamic model based safety analysis of a three-phase catalytic slurry intensified continuous reactor

S. Li, S. Bahroun, C. Valentin, C. Jallut, F. de Panthou

Dynamic model based safety analysis of a three-phase catalytic slurry intensified continuous reactor

S. Li[1], S. Bahroun[1], C. Valentin[1*], C. Jallut[1], F. De Panthou[2]

1 Université de Lyon, F-69622 Lyon, France ; Université Lyon 1, Villeurbanne ;

LAGEP, UMR 5007, CNRS, CPE, Bât308G, 43 boulevard du 11 Novembre 1918,

69100 Villeurbanne, France ;

{lis, bahroun, valentin, jallut}@lagep.univ-lyon1.fr

2 AETGROUP SAS, 6 montée du Coteau, 06800 Cagnes-sur-mer, France ;

fabrice.depanthou@aetgroup.com

[*] *Corresponding author: C. Valentin, e-mail: valentin@lagep.univ-lyon1.fr, Tel: (+33) 4 72 43 18 66, Fax: (+33) 4 72 43 16 82.*

Abstract

Safety analysis like the HAZOP (HAZard OPerability) study can be much more efficient if a dynamic model of the system under consideration is available to evaluate the consequences of hazard deviations and the efficiency of the proposed safety barriers. In this paper, a dynamic model of a three-phase catalytic slurry intensified continuous chemical reactor is used within the context of its HAZOP (HAZard OPerability) study. This reactor, the RAPTOR®, is an intensified continuous mini-reactor designed by the French company AETGROUP SAS that can replace batch or fed-batch processes in the case of highly exothermic reactions involving hazardous substances. The highly hazardous hydrogenation of o-cresol under high pressure and temperature is taken as an example of application. Deviations as a temperature increase of the cooling medium or no cooling medium flow can produce an overheating of the reactor. Thus, three possible safety barriers are evaluated by simulation: shut off the gaseous reactant feed, shut off the liquid reactant feed or stop the agitation. The more efficient actions are the stopping of the agitation and/or of the gas reactant feed. The simulation results can efficiently help the reactor design and optimisation. Safety analysis can also be one of the criteria to compare batch and intensified continuous processes.

Keywords: dynamic modelling; HAZOP; safety analysis; three-phase catalytic reactor; intensified continuous reactor

1. Introduction

The main tools to perform hazardous chemical synthesis in the field of fine chemicals and pharmaceuticals remain the batch reactors. However, even if they offer the required flexibility and versatility, they present a number of technological limitations. In particular, due to their poor heat transfer performances, the heat generated by exothermic chemical reactions is a serious problem with regard to safety. To overcome this problem, solvents are used to reduce chemical rates by dilution and to absorb a part of the energy involved in the chemical reactions. The use of the fed-batch mode is also a way to control the course of the chemical reaction by controlling the feed rate.

An alternative approach is allowed by the recent evolution of process intensification and the mini/micro reactors development. The idea is to perform the reactions in tubular reactors having high heat and mass transfer performances. This transition from batch to continuous processes can be based on several advantages of the continuous intensified mini-reactors when compared with the batch reactor (Lomel et al., 2006):

- a better control of heat exchange allowing to concentrate the reactants and thus limiting the amount of solvent to be treated;
- a better performance and a higher selectivity.

Another way to compare batch and continuous intensified processes is the consideration of safety issues. Process intensification can lead to inherently safer design, particularly by lowering chemicals instantaneous inventories (Etchells, 2005).

In the safety analysis, hazard and operability studies are methodologies for identifying and dealing with potential problems in industrial processes, particularly those that would create a hazardous situation or severe damages in the process or for the operators. It is commonly known as HAZOP (HAZard OPerability) (Laurent, 2003), and is said to be the most widely used method of hazard analysis in the process industries (Gould, 2000), notably the chemical, petrochemical and nuclear industries. A history of HAZOP analysis can be found in Kletz (2006). A multidisciplinary team consisting of five or more members led by a team leader usually carries out HAZOP studies. The process is decomposed into small sections, such as individual equipments or pipes. The HAZOP team systematically considers the possible significant deviations of state variables (flow rate, pressure, temperature, level, composition) by using guide words including “NONE”, “MORE”, “LESS”, “REVERSE”, “OTHER THAN”, “PART OF”, etc.

The consequences of these deviations are analysed with respect to hazard, then the possible causes are identified and achievable actions are proposed.

In some cases, particularly for chemical reactors, the HAZOP team cannot find relevant consequences and corresponding corrective actions for some hazardous deviations. A model assisted safety analysis can be considered by performing dynamic stability studies (Zaldivar *et al.*, 2003) or numerical simulations to find out the right actions (Svandova *et al.*, 2005; Eizenberg *et al.*, 2006; Rizal *et al.*, 2006; Benaissa *et al.*, 2008). Dynamic simulations are necessary since deviations or sudden problems lead to transient evolutions of the process.

In this article, a dynamic model of a three-phase catalytic slurry intensified continuous reactor is proposed. It is shown how such a model can help to perform a HAZOP study. Important potential hazardous cases can be simulated:

- "MORE", "LESS" and "NO" reactant feed and cooling medium flow;
- "MORE" and "LESS" temperature of reactant feed and cooling medium feed.

The simulation results are used to find out the appropriate actions in the HAZOP study. Such a model may also be very useful for automatic control. As a matter of fact, among new safety problems that can arise if intensified processes are used, it is pointed out that control and monitoring may be more difficult (Etchells, 2005). Because of these innovating features, the intensified reactors require developing specific tools in the fields of control, modelling and simulation.

The heterogeneous catalytic o-cresol hydrogenation is taken as an interesting test example to illustrate the method. It is assumed to be representative of many highly hazardous industrial situations. Chemical rates and thermodynamic data are available in the literature for this reaction (Hichri *et al.*, 1991).

2. Dynamic Model description

2.1. A continuous three-phase catalytic slurry intensified chemical reactor

Fig. 1 shows the RAPTOR®, an intensified stirred continuous reactor designed by AETGOUP SAS Company, a French society whose main activity is focused on chemical process industrialisation and continuous process technology. This reactor is particularly efficient for reactions with mass transfer limitations (liquid/liquid, gas/liquid, gas/liquid/solid). Process intensification may require extreme

conditions of pressure and temperature in order to have complete reaction within a few minute residence time (RAPTOR® is thus designed up to 300°C and 250 bar). The RAPTOR® is also large enough to handle solids. As a consequence, hydrogenations involving a dispersed catalyst in a slurry are of particular interest to be tested with this continuous technology. For confidentiality reasons, a detailed description of the RAPTOR® cannot be given.

2.2. The three-phase catalytic chemical reaction

The heterogeneous catalytic hydrogenation of o-cresol stœchiometry is as follows:

$$3H_2 + C_6H_4OHCH_3 \overset{catalyst}{\rightarrow} C_6H_{10}OHCH_3 \quad (1)$$

or

$$\nu_A A_g + \nu_B B_l \rightarrow \nu_C C_l \quad (2)$$

The observations realized during industrial reactions performed at a working temperature between 200°C and 300°C and a very high hydrogen working pressure of 200 bar show that the reverse dehydrogenation reaction that would lead to a possible equilibrium is negligible. Such an assumption is very common for the o-cresol hydrogenation reaction, even at more conventional working conditions (Zwicky *et al.*, 1978; Hichri *et al.*, 1991; Vasco de Toledo *et al.*, 2001) as well as for liquid or gaseous phase hydrogenation of other hydrocarbons (Kadivar *et al.*, 2009; Schweitzer *et al.*, 2010). The reaction occurs between the dissolved hydrogen and liquid o-cresol in presence of the catalyst deposited on the surface of a dispersed porous solid (Ramachandran and Chaudhari, 1983; Wärnä and Salmi, 1996). The chemical process involves several steps in series (see fig. 2):

- hydrogen absorption at the gas-liquid interface;
- hydrogen transfer from gas-liquid interface to the bulk liquid;
- hydrogen and o-cresol transfer from bulk liquid through liquid-solid interface;
- intraparticle diffusion of hydrogen and o-cresol;
- adsorption of the reactants on the catalyst surface;
- adsorbed phase reaction.

Langmuir-Hinshelwood model represents in a realistic way the adsorption phenomena involved in heterogeneous catalysis processes. The reaction rate for reaction (2) is calculated by equation (3):

$$R = k\frac{K_A K_B C_{As} C_{Bs}}{(1+K_A C_{As})(1+K_B C_{Bs})} \quad (3)$$

where C_{As} and C_{Bs} are respectively the hydrogen and o-cresol concentrations within the catalyst pores.

This kinetic model has been selected by Hichri *et al.* (1991) among the classical ones that are chosen for the situation under consideration since it is the one leading to the best fits of their experimental data. The global reaction rate (3) is derived by using the steady-state assumption for some intermediates of the proposed mechanism. Since we propose a dynamic modelling of a chemical reactor, this assumption may be questionable but we consider that in our case, due to the time constant of the system that we consider, the kinetic model (3) can be applied. As a matter of fact, this kinetic model applied to o-cresol hydrogenation has been extensively used for the dynamic modelling of three-phase catalytic slurry reactors (Vasco de Toledo *et al.*, 2001). Vasco de Toledo *et al.* (2001) show transient state non isothermal simulations of a three-phase catalytic slurry reactor with durations of about 500 s. The transient behavior that we obtain here is similar. Furthermore, Hichri *et al.* (1991) perform transient isothermal semi-batch experiments for different temperatures that are very well represented by the equation (3). The duration of these experiments are about 6000 s.

The Arrhenius law gives the variation of the rate constant k with temperature while adsorption constants K_A and K_B variations derive from mass action law. The following expressions have been established in Hichri *et al.* (1991):

$$k = 5,46.10^{8}\exp(-82220/RT_s) \quad (4)$$

$$K_A = 10,55.10^{-3}\exp(+5003/RT_s) \quad (5)$$

$$K_B = 7,54.10^{-6}\exp(+16325/RT_s) \quad (6)$$

where T_s is the catalyst pellet temperature that is assumed to be uniform within the pellet.

2.3. Dynamic model

Due to the presence of the stirrer, the tubular continuous intensified reactor is treated as an association of J perfectly stirred tank reactors in series with back mixing effect represented by the parameter α. This flow model is assumed to hold for the three phases of the slurry: the liquid phase, the gaseous phase and the catalyst. Similarly, the jacket content is treated as the association of J perfectly

stirred tank reactors in series, as shown in fig. 3 (Bahroun *et al.*, 2009). In order to take into account the influence of the reactor metallic body, *J* pieces of the metal body are also included in the description of the system, the temperature of each being assumed to be uniform. Such an influence of the reactor body has been emphasized in the case of heat-exchanger reactors for example (Benaissa *et al.*, 2008).

The following assumptions are also considered to derive the dynamic model (Santana *et al.*, 2001; Vasco de Toledo *et al.*, 2001; Bahroun *et al.*, 2009):

- the temperature of the liquid and gas phases are assumed to be equal;
- a global mass transfer coefficient is used to represent hydrogen transfer from the liquid surface to the bulk. Equilibrium conditions at the gas-liquid interface are assumed;
- the pressure drop is negligible;
- the resistances to mass and heat transfer at the catalyst pellet surface and within the pores are lumped into global heat and mass transfer coefficients;
- the material balance in the gas phase, that is assumed to be pure hydrogen, is written at steady state;
- the gaseous phase is assumed to be ideal.

The model consists in material and energy balance equations for the gaseous phase, the liquid-bulk phase and the catalyst particles, and also energy balance for the metal body and the cooling medium in the jacket. These balances are written for each stirred tank reactor used for the representation of the bulk flow, the jacket liquid flow and the corresponding piece of metal body according to an approach that has been applied to other reactive processes (Choulak *et al.*, 2004). The *k* index is used to designate this set of three finite volumes at a given axial position of the reactor (see fig. 3).

The bulk volume of the k^{th} discretization element V_k is divided into the liquid phase volume $\varepsilon_l^k V_k$, the catalyst volume $\varepsilon_s V_k$ and the gaseous phase volume $\varepsilon_g^k V_k$. As the gas is consumed by the reaction, the gas phase hold-up $\varepsilon_g^k V_k$ as well as the volumetric surface area of the gas-liquid interface a_{gl}^k are assumed to vary with the axial position while the amount of catalyst $\varepsilon_s V_k$ remains constant. The net volumetric flow rates of the liquid and catalyst phases are respectively denoted as q_l and q_s, and are assumed to be constant. Due to the hydrogen consumption, the gaseous phase volumetric flow rate varies with the axial position: it is denoted as q_g^k. The dynamic part of the model is given by the following balance equations (7) to (14). They are written for each discretization element *k* (see figure 3):

Mass balance of reactant A (hydrogen):

liquid phase

$$\varepsilon_l^k V_k \frac{dC_{Al}^k}{dt} = (1+\alpha) q_l C_{Al}^{k-1} + \alpha q_l C_{Al}^{k+1} - (1+2\alpha) q_l C_{Al}^k \\ - V_k k_{ls,A} a_{ls} \left(C_{Al}^k - C_{As}^k\right) + V_k k_{gl,A} a_{gl}^k \left(C_{Al}^{*k} - C_{Al}^k\right) \quad (7)$$

solid phase

$$\varepsilon_s V_k \frac{dC_{As}^k}{dt} = (1+\alpha) q_s C_{As}^{k-1} + \alpha q_s C_{As}^{k+1} - (1+2\alpha) q_s C_{As}^k \\ + V_k k_{ls,A} a_{ls} \left(C_{Al}^k - C_{As}^k\right) - \nu_A \varepsilon_s \rho_s V_k R(C_{As}^k, C_{Bs}^k, T_s^k) \quad (8)$$

The hydrogen solubility at the gas-liquid interface is calculated by using the Henry constant that is available in Hichri *et al.* (1991):

$$C_{Al}^{*k} = \frac{P}{11538 \exp\left(\frac{4990}{RT_f^k}\right)} \quad (9)$$

Mass balance of reactant B (o-cresol):

liquid phase

$$\varepsilon_l^k V_k \frac{dC_{Bl}^k}{dt} = (1+\alpha) q_l C_{Bl}^{k-1} + \alpha q_l C_{Bl}^{k+1} \\ - (1+2\alpha) q_l C_{Bl}^k - V_k k_{ls,B} a_{ls} (C_{Bl}^k - C_{Bs}^k) \quad (10)$$

solid phase

$$\varepsilon_s V_k \frac{dC_{Bs}^k}{dt} = (1+\alpha) q_s C_{Bs}^{k-1} + \alpha q_s C_{Bs}^{k+1} - (1+2\alpha) q_s C_{Bs}^k \\ + V_k k_{ls,B} a_{ls} (C_{Bl}^k - C_{Bs}^k) - \nu_B \varepsilon_s \rho_s V_k R(C_{As}^k, C_{Bs}^k, T_s^k) \quad (11)$$

Energy balance in the fluid (both gas and liquid) phase:

$$V_k \left(\varepsilon_g^k \rho_g C_{pg} + \varepsilon_l^k \rho_l C_{pl}\right) \frac{dT_f^k}{dt} = hS\left(T_m^k - T_f^k\right) + V_k h_s a_{ls} (T_s^k - T_f^k) \\ + \rho_g C_{pg} \left((1+\alpha) q_g^{k-1} T_f^{k-1} + \alpha q_g^{k+1} T_f^{k+1} - (1+2\alpha) q_g^k T_f^k\right) \\ + \rho_l C_{pl} \left((1+\alpha) q_l T_f^{k-1} + \alpha q_l T_f^{k+1} - (1+2\alpha) q_l T_f^k\right) \quad (12)$$

Energy balance in the solid phase:

$$\varepsilon_s V_k \rho_s C_{ps} \frac{dT_s^k}{dt} = V_k h_s a_{ls} (T_f^k - T_s^k) \\ + \rho_s C_{ps} \left((1+\alpha) q_s T_s^{k-1} + \alpha q_s T_s^{k+1} - (1+2\alpha) q_s T_s^k\right) \\ - \varepsilon_s V_k \rho_s \Delta H_r R(C_{As}^k, C_{Bs}^k, T_s^k) \quad (13)$$

Energy balance of the metal body of the mini-reactor :

$$V_{mk}\,\rho_m C_{pm}\,\frac{dT_m^{\,k}}{dt} = hS_k\left(T_f^{\,k} - T_m^{\,k}\right) + h_j S_k\left(T_j^{\,J-k+1} - T_m^{\,k}\right) \tag{14}$$

Energy balance of the cooling medium in the jacket :

$$V_{kj}\rho_j C_{pj}\,\frac{dT_j^k}{dt} = h_j S_k\left(T_m^{J-k+1} - T_j^k\right) - \rho_j C_{pj} q_j^{k-1}\left(T_j^k - T_j^{k-1}\right) \tag{15}$$

In order to take into account the gaseous phase hydrogen consumption, the steady-state hydrogen mass balance is written according to equation (16) for the k^{th} reactor:

$$(1+2\alpha)\varepsilon_g^k S_T J_{Ag} + V_k k_{gl,A} a_{gl}^k\left(C_{Al}^{k*} - C_{Al}^k\right) = (1+\alpha)\varepsilon_g^{k-1} S_T J_{Ag} + \alpha\varepsilon_g^{k+1} S_T J_{Ag} \tag{16}$$

with :

$$\varepsilon_g^k = N_b^k\,\frac{4}{3}\pi r_b^3 / V_k \tag{17}$$

$$a_{gl}^k = N_b^k\,4\pi r_b^2 / V_k \tag{18}$$

The equations (16)-(18) allow calculating spherical bubbles number $N_b^{\,k}$ in the k^{th} reactor by assuming constant bubbles radius r_b and constant gas molar flux J_{Ag}. Then, the spatial evolution of the gaseous volumetric hold-up $\varepsilon_g^k V_k$ as well as that of the gas-liquid interface surface area a_{gl}^k and the gas volumetric flow rate in the k^{th} reactor $q_g^{\,k}$ are straightforward.

2.4. Steady-state sensitivity analysis to some transfer parameters

Since the RAPTOR® is a completely new and confidential system, no semi empirical correlations are available to calculate the heat and mass transfer coefficients. We have taken the values of these transfer coefficients between the bulk and the catalyst surface in the open literature (Vasco de Toledo *et al.*, 2001) and performed a sensitivity analysis of the model with respect to these parameters. Only the inlet gas-liquid mass transfer $k_{gl,A}a_{gl}^0$ and the heat transfer coefficients between the reactor body and the bulk as well as the cooling medium, respectively h and h_j, turn to be really sensitive. The model steady-state behavior has been determined from steady-state experimental data corresponding to the nominal operation of a small-scale pilot of the RAPTOR®. In this case, an o-cresol conversion of *98.23%* is obtained and bulk temperature increase between the reactor inlet and outlet is *102.4°C*. One can see on figures 4 and 5 the results of a sensitivity study of the model steady-state behavior when these parameters vary of ±20% from their nominal values. Temperature and conversion vary less than ±20% (between 3%

to 20%). As far as safety analysis is concerned, the conclusions that can be drawn from numerical simulations may naturally depend on the precision of the heat and mass transfer coefficients (Svandová *et al.*, 2008).

3. Case studies by model simulations

3.1. Steady-state simulations for sensitivity analysis to operating conditions

The operating point of the reactor under consideration corresponds to the nominal operation of a small-scale pilot of the RAPTOR® with a working volume of 242 ml. A slurry made of catalyst dispersed in liquid o-cresol is fed into the reactor with hydrogen at 200 bar. The cooling medium jacket inlet temperature is 165°C. The inlet gaseous phase volumetric fraction is 47.5%. A temperature constraint is that the metal body temperature cannot exceed 250°C (50 °C below construction limitation). The materials that are used for the gaskets impose this constraint. No more information can be given about this confidential equipment. First the steady-state behaviour of the continuous intensified reactor is studied.

Fig. 6 presents the axial variations of the temperatures, the conversion and the gaseous phase hold-up at the nominal operating point. The conversion is defined with respect to the o-cresol.

Fig. 7 gives the variations of the conversion and the reactor temperatures at the outlet axial position according to the o-cresol flow rate. The highest productivity with high purity of the product (over 99%) is obtained for an o-cresol flow rate comprised between 0.3 and 0.4 $ml.s^{-1}$. If more o-cresol is fed, the quality of the product can no more be guaranteed, but the metal body temperature does not exceed the constraint.

The o-cresol inlet temperature has a great influence on the conversion, as shown in fig. 8. A satisfying conversion is obtained only if the o-cresol inlet temperature is greater then 160 °C.

In fig. 9, the variation of temperature and conversion as a function of the gas inlet volumetric flow rate is presented. The temperature and the conversion increase firstly with the gas flow rate because more gas reactant is available for the reaction. But if the gas flow rate continues to increase, the reactor is cooled and the conversion is decreased.

The jacket is fed with a relatively very high flow rate of cooling medium compared with the reactant flow rate inlet. Hence the variation of the cooling medium flow rate inlet has little effect on the reactor

outlet. On the contrary, the influence of the cooling medium inlet temperature on the reactor outlet is great as it can be seen in fig. 10, the cooling medium inlet temperature ranging from 80°C to 220°C. The metal temperature exceeds 250°C when the cooling medium inlet temperature is above 200°C.

3.2. Evaluation of the consequences of hazardous events: dynamic simulations

3.2.1 "NO COOLING MEDIUM" hazardous event

In the case of exothermic reactions, one of the most important problems in the safety analysis is to guarantee a correct running of cooling system. In fig. 11, the consequence of the event "NO COOLING MEDIUM" occurring at t=500 s has been simulated. It can be seen that the metal body temperature increases rapidly and exceeds 250°C after only 165 seconds. It outlines the safe behaviour of this equipment because current technology (PLCs, controllers, ...) can act in much less time.

Three possible actions are proposed in order to stop the chemical reaction:

- shutting off the gas reactant inlet;
- shutting off the liquid reactant inlet;
- stopping the agitation to highly decrease the gas-liquid mass transfer efficiency.

In fig. 12, the three corrective actions are compared. They are applied at t=665 s, when the metal body temperature reaches the constraint value of 250°C (imposed especially by the gaskets). The actions of stopping the agitation and shutting off the gas reactant inlet flow are the best ones. They have the immediate effect of causing the temperature decrease. In a fed-batch reactor, when such an exothermic effect is detected, it can be too late, due to mass and thermal inertia. Even if detected early, the corrective action may be too late to prevent thermal runaway. On the contrary, in a continuous mini-reactor, even with a late detection, action instantly safely corrects the deviation. Shutting off the liquid flow rate does not eliminate the great overshoot because of the amount of liquid in the reactor.

3.2.2 "COOLING MEDIUM INLET TEMPERATURE INCREASE" hazardous event

One hazard deviation of the cooling system is the fail of temperature regulation of the external cooling heat exchanger. This event leads the cooling medium inlet temperature increasing above the safety range.

In fig. 13, the consequences of a sudden increase of the cooling medium temperature from 165°C to 210°C at t=500 s are given. The metal temperature exceeds 250°C after about 378 s and then remains constant equal to 253°C. A good heat transfer is highlighted. The effects of the same three corrective actions are compared in the fig. 14. As in the previous deviation, stopping the agitation and shutting off gas inlet flow rate remain the best actions to perform and have the immediate effect of causing the decrease of temperature.

3.2.3 The metal reactor body mass as an inherent safety characteristic

Due to their high surface/volume ratio, the intensified reactors also present a high (reactor mass)/(bulk mass) ratio. This characteristic is interesting with respect to runaway situations (Benaissa *et al.*, 2008). In intensified continuous reactors, the metal body of the reactor plays the same role as the one of the solvent used for operating the batch or fed-batch reactor: it allows accumulating the energy that is released by the chemical reaction.

If even greater safety margins are required, the metal body volume could be increased to make this intensified reactor even safer. In fig. 15, three dynamic simulations with different metal body volume are compared when the “NO COOLING MEDIUM” event occurs at 500 s. The time delay to reach the reactor runaway as defined by the temperature constraint for the metal body and its gaskets (T_m < 250°C) increases if the metal body volume increases. For respectively, V_m, $2V_m$ and $3V_m$, the runaway time is equal to 164.9 s, 337.4 s and 512 s. The current choice, taking into account pressure, temperature and mechanical constraints, is very relevant and allows the operators and the control system to have a sufficient time delay to take a safety strategy. This thickness has however to be compatible with the steady-state heat flux necessary to maintain adequate temperature in the reactor.

4. Conclusion

In this paper, dynamic simulations are used as a tool for safety study of an intensified continuous stirred reactor. This reactor is particularly efficient for reactions with mass transfer limitations (liquid/liquid, gas/liquid, gas/liquid/solid) mainly due to the internal stirring system. Thanks to its high surface/volume ratio compared to batch processes, it is also very effective for heat exchange. Since process intensification may require extreme pressure and temperature conditions, the RAPTOR® is

designed to work up to 300°C and 300 bar as well as to handle solids. Thus the heterogeneous catalytic o-cresol hydrogenation is an interesting test example for this intensified continuous technology. The steady-state behaviour of the intensified continuous reactor is firstly studied by simulation. Then, the consequences of deviations of flow rate and temperature of the cooling medium are simulated within the framework of a safety analysis. A very simple corrective action consisting in stopping the agitation turns out to be the most efficient for the relevant hazard situations that have been considered and has the immediate effect of causing the decrease of temperature. Contrary to what one might think, it is more efficient than the gas shut off. The efficient stirring system is thus probably the reason of the availability of a lot of solubilized hydrogen in the organic media under the operating conditions. It means that, with this technology, the kinetic limitation is no more the solubilization of hydrogen, which is generally considered in usual batch reactors. Therefore it is not surprising that, from the safety point of view, it is better to stop mixing in order that the value of the mass transfer coefficient falls down. Then, the concentration of hydrogen in liquid phase decreases very quickly close to zero and the reaction is stopping. Another interesting inherent safety characteristic of the reactor under consideration is its high (metal body mass)/(bulk mass) ratio. This characteristic is dynamically favourable since it allows an accumulation of the heat released by the chemical reaction during possible runaway situations.

All these simulations outline the safe behaviour of this equipment because current technology (PLCs, controllers...) and operators have the time to act well before the thermal runaway could happen.

Acknowledgement

This project devoted to intensification of fine chemicals workshop is supported by the French research agency ANR (Agence Nationale de la Recherche).

Nomenclature

a_{gl} and a_{ls}	gas-liquid and liquid-solid interfacial areas respectively, m^2/m^3
C_A	concentration of the component A, $mol.m^{-3}$
C_A^*	solubility of the component A, $mol.m^{-3}$
C_B	concentration of the component B, $mol.m^{-3}$
C_p	heat capacity, $J.K^{-1}.kg^{-1}$
F	molar flow rate, $mol.s^{-1}$
He	Henry's constant, $Pa.m^3.mol^{-1}$
h	heat transfer coefficient, $W.m^{-2}.K^{-1}$
J	Molar flux, $mol.\ m^{-2}.s^{-1}$
K	adsorption constant, $m^3.mol^{-1}$
k	kinetic constant, $mol.kg^{-1}.s^{-1}$
k_{gl} and k_{ls}	gas-liquid and liquid-solid mass transfer coefficients respectively, $m.s^{-1}$
N_b	hydrogen bubbles number
P	pressure, Pa
q	volumetric flow rate, $m^3.s^{-1}$
R	reaction rate, $mol.kg^{-1}.s^{-1}$
r_b	hydrogen bubble radius, m
S	surface, m^2
S_T	surface of reactor section, m^2
T	temperature, K
V	volume, m^3

Greek symbols

$\Delta_r H$	heat of reaction, $J.mol^{-1}$
v	stoichiometric coefficient
α	back mixing coefficient
ρ	mass density, $kg.m^{-3}$

ε_g	gas hold-up
ε_l	liquid hold-up
ε_s	solid hold-up

Subscripts

A	component A
B	component B
j	jacket fluid
f	fluid
g	gas
k	reactor number
l	liquid
m	metal body
s	solid catalyst

Superscripts

I	Inlet
k	reactor number
O	Outlet

References

Bahroun S, Jallut C, Valentin C, De Panthou F. Dynamic modelling of a three-phase catalytic slurry intensified chemical reactor. IFAC Symposium on Advanced Control of Chemical Processes (ADCHEM), July 12-15, Istanbul, Turkey 2009: 862-7.

Benaissa W, Gabas N, Cabassud M, Carson D, Elgue S, Demissy M. Dynamic behaviour of a continuous heat exchanger/reactor after flow failure. Journal of Loss Prevention in the Process Industries 2008; 21: 528-536.

Choulak S, Couenne F, Le Gorrec Y, Jallut C, Cassagnau P, Michel A. A generic dynamic model for simulation and control of reactive extrusion. IEC Res. 2004; 43(23): 7373-82.

Eizenberg S, Shacham M, Brauner N. Combining HAZOP with dynamic simulation – Application for safety education. Journal of Loss Prevention in the Process Industries 2006; 19: 754-761.

Etchells JC. Process intensification. Safety Pros and Cons. Process Safety and Environmental Protection 2005; 83(B2): 85-9.

Gould J. Review of Hazard identification techniques. HSE; 2000. (http://www.hse.gov.uk/research/hsl_pdf/2005/hsl0558.pdf).

Hichri H, Armand A, Andrieu J. Kinetics and slurry-type reactor modelling during catalytic hydrogenation of o-cresol on Ni/SiO2. Chemical Engineering Process 1991; 30: 133–140.

Kadivar A, Sadeghi MT, Sotudeh-Gharebagh R, Mahmudi M. Estimation of kinetic parameters for hydrogenation reactions using a genetic algorithm. Chem. Eng. Technol. 2009; 32: 1588-94.

Kletz T. Hazop and Hazan. 4th ed. Institution of Chemical Engineers (IChemE); 2006.

Laurent A. Sécurité des procédés chimiques – connaissances de base et méthodes d'analyse de risques. Tec & Doc Lavoisier ; 2003.

Lomel S, Falk L, Commenge JM, Houzelot JL, Ramdani K. The microreactor. A systematic and efficient tool for the transition from batch to continuous process. Chemical Engineering Research and Design 2006; 84(A5): 363-9.

Ramachandran P, Chaudhari RV. Three-phase catalytic reactors. Gordon and Breach, New York. 1983.

Rizal D, Tani S, Nishiyama K, Suzuki K. Safety and reliability analysis in a polyvinyl chloride batch process using dynamic simulator-case study: loss of containment incident. Journal of Hazardous Materials 2006; A137: 1309-20.

Santana PL, Vasco de Toledo EC, Meleiro LAC, Scheffer R, Freitas Jr. NB, Maciel MRW et al. A Hybrid mathematical model for a three-phase industrial hydrogenation reactor. European symposium on computer aided process engineering, Kolding, Denmark 2001; 11: 279–284.

Schweitzer JM, Lopez-Garcia C, Ferré D. Thermal runaway analysis of a three-phase reactor for LCO hydrotreatment. Chemical Engineering Science 2010; 65: 313-321.

Svandová Z, Jelemenský L, Markos J, Molnar A. Steady states analysis and dynamic simulation as a complement in the HAZOP study of chemical reactors. Process Safety and Environmental Protection 2005; 83(B5): 463-471.

Svandová Z, Markos J, Jelemenský L. Impact of Mass Transfer Coefficient Correlations on Prediction of Reactive Distillation Column Behaviour. Chemical Engineering Journal 2008; 140: 381 – 390.

Vasco de Toledo EC, Santana PL, Maciel MRW, Maciel Filho R. Dynamic modelling of a three-phase catalytic slurry reactor. Chemical Engineering Science 2001; 56: 6055–61.

Wärnä J, Salmi T. Dynamic modelling of catalytic three phase reactors. Computers in Chemical Engineering 1996; 20: 39–47.

Zaldivar JM, Cano J, Alos MA, Sempere J, Nomen R, Lister D, Maschio G., Obertopp T., Gilles ED, Bosch J, Strozzi F. A general criterion to define runaway limits in chemical reactors. Journal of Loss Prevention in the Process Industries 2003; 16: 187-200.

Zwicky JJ, Gut G. Kinetics, poisoning and mass transfer effects in liquid-phase hydrogenations of phenolics compounds over a palladium catalyst. Chemical Engineering Science 1978; 33: 1363-9.

Fig. 1. The “RAPTOR®” (« **R**éacteur **A**gité **P**olyvalent à **T**ransfert **O**ptimisé **R**ectiligne » in french).

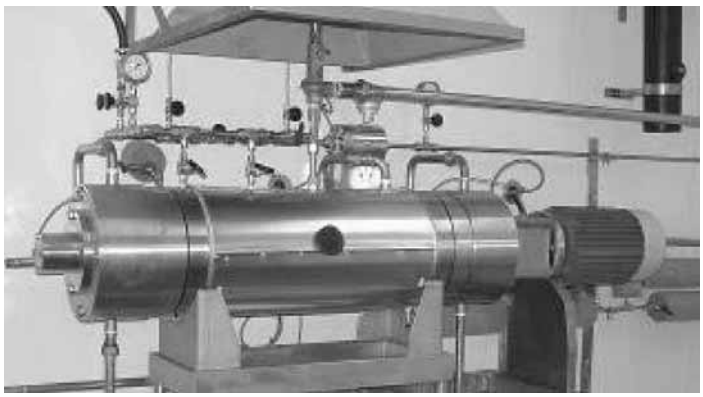

Fig. 2. Steps of the catalytic reaction (Bahroun et al., 2009).

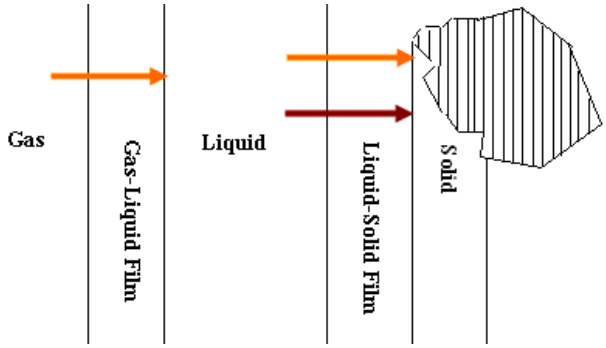

Fig. 3. Spatial discretization of the mini-reactor (Bahroun et al., 2009).

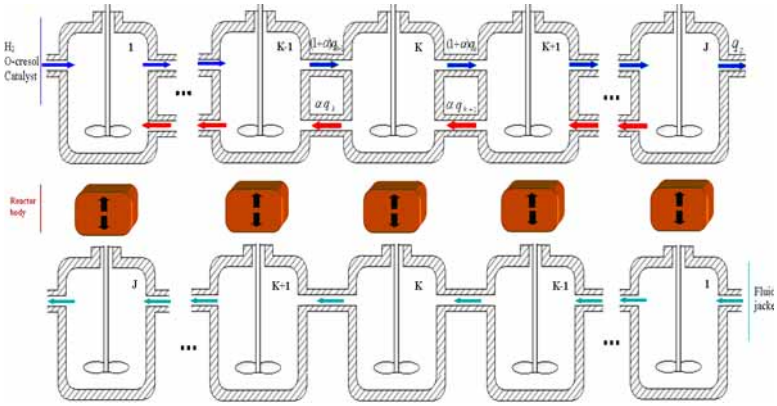

Fig. 4. Temperature and conversion at the reactor outlet axial position as a function of gas-liquid mass transfer coefficient ($k_{gl,A}a_{gl}^{0}$).

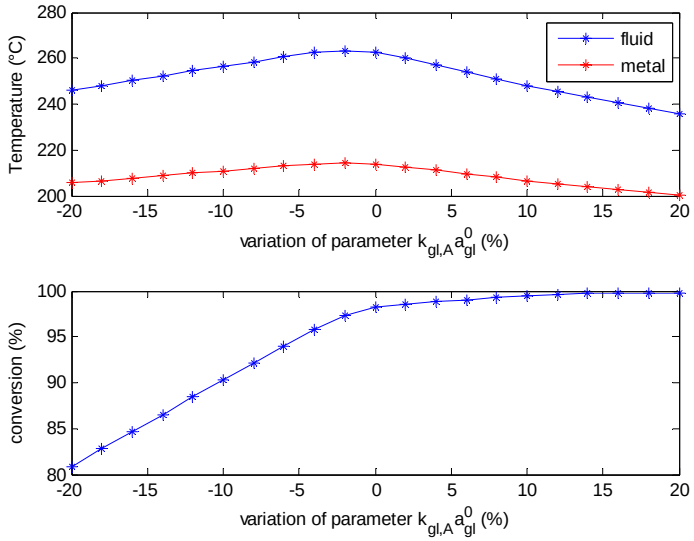

Fig 5. Temperature and conversion at the reactor outlet axial position as a function of heat transfer coefficient (h and h_j).

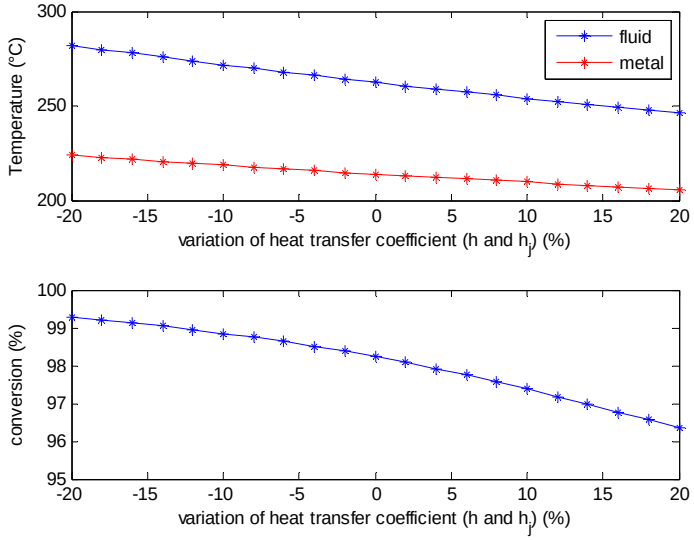

Fig. 6. Temperature, conversion and gaseous phase hold-up profiles for the nominal operating point.

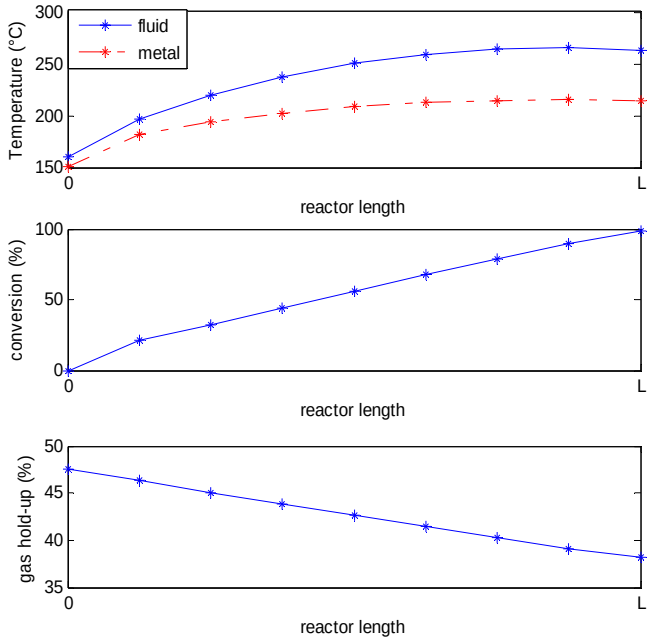

Fig. 7. Temperature and conversion at the reactor outlet axial position as a function of o-cresol inlet flow rate.

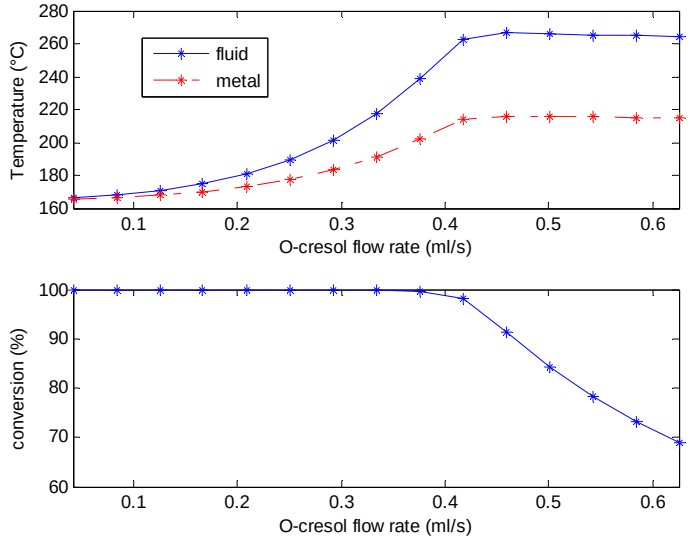

Fig. 8. Temperature and conversion at the reactor outlet axial position as a function of o-cresol inlet temperature.

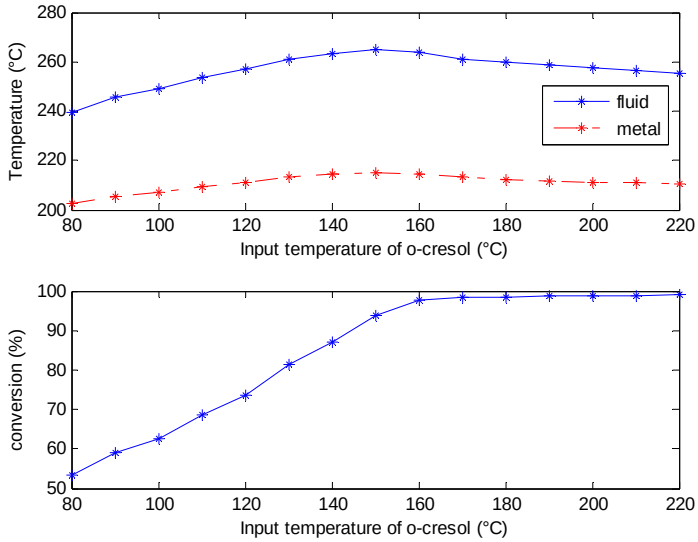

Fig. 9. Temperature and conversion at the reactor outlet axial position as a function of hydrogen inlet flow rate**.**

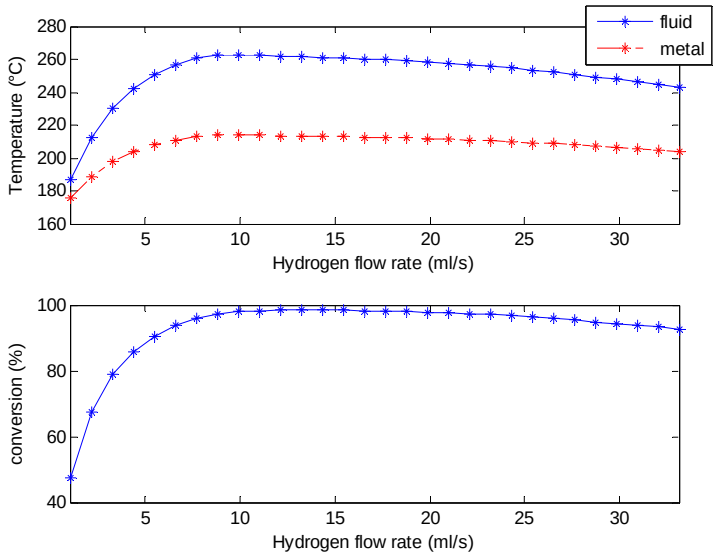

Fig. 10. Temperature and conversion at the reactor outlet axial position as a function of the inlet cooling medium temperature.

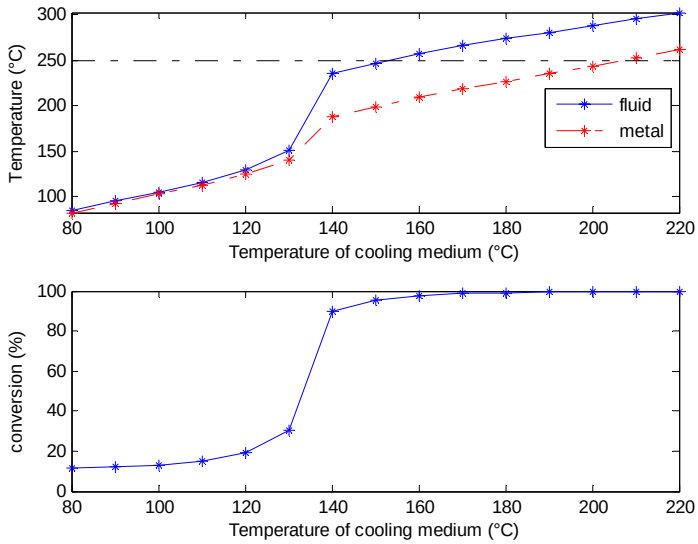

Fig. 11. Metal body temperature evolution after the "NO COOLING MEDIUM" event occurring at 500 s.

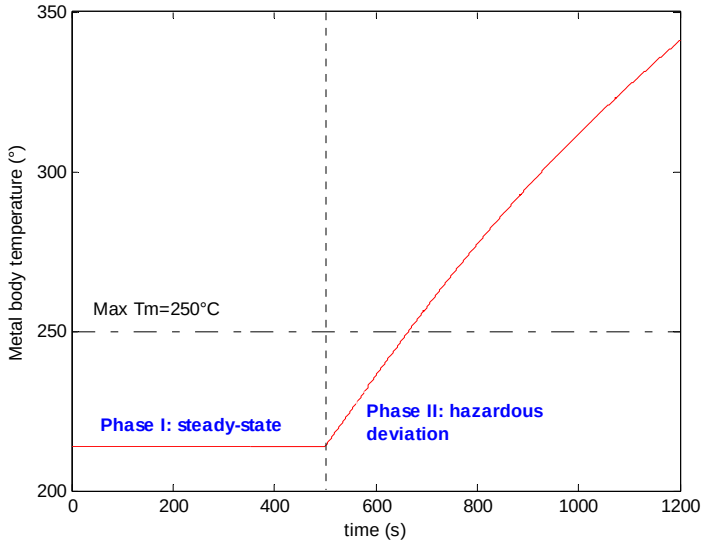

Fig. 12. Consequences of the corrective actions after the “NO COOLING MEDIUM” event.

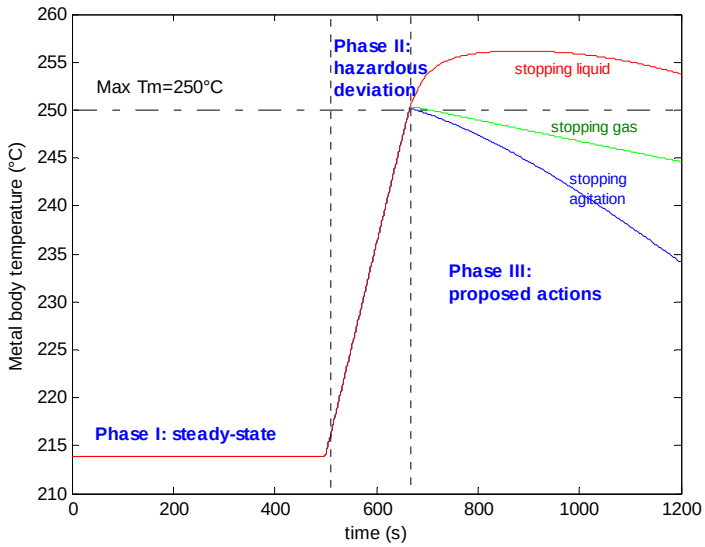

Fig. 13. Metal body temperature after the “COOLING MEDIUM INLET TEMPERATURE 45 °C INCREASE” event at 500 s.

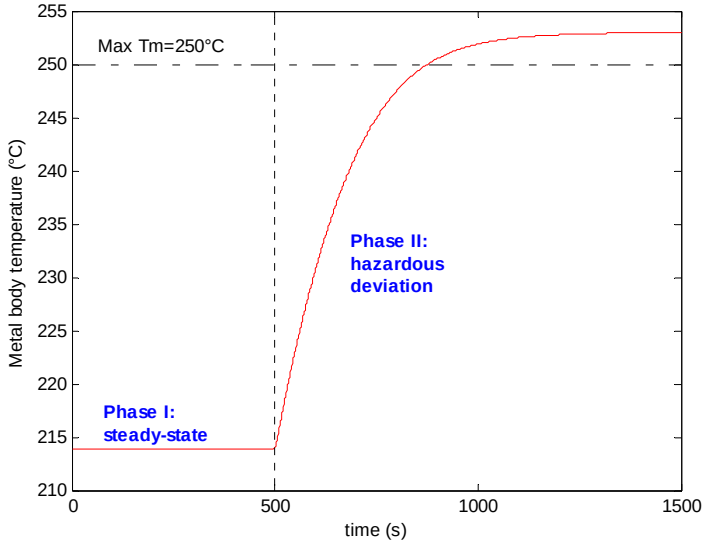

Fig. 14. Consequences of the corrective actions after the “COOLING MEDIUM INLET TEMPERATURE 45 °C INCREASE” event.

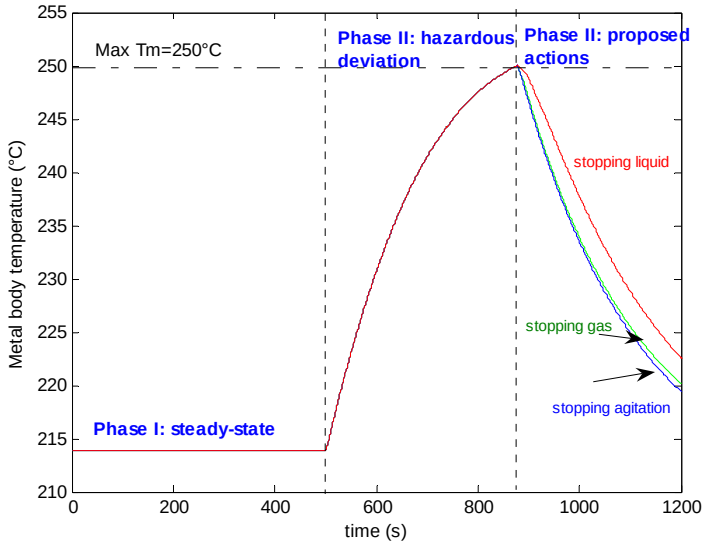

Fig. 15. Metal body temperature evolution after the “NO COOLING MEDIUM” event occurring at 500 s with three different metal body volumes: V_m, $2V_m$, $3V_m$.